Proc. Natl. Acad. Sci. USA
Vol. 93, pp. 7283–7288, July 1996
Medical Sciences

Spontaneous diabetes mellitus in transgenic mice expressing human islet amyloid polypeptide

JULIETTE JANSON*, WALTER C. SOELLER†, PATRICK C. ROCHE‡, ROBIN T. NELSON†, ANTHONY J. TORCHIA†, DAVID K. KREUTTER†, AND PETER C. BUTLER*§

*Endocrine Research Unit, ‡Department of Laboratory Medicine and Pathology, Mayo Clinic, Rochester, MN 55905; and †Pfizer Inc., Central Research Division, Groton, CT 06340

Communicated by Donald F. Steiner, University of Chicago, Chicago, IL, April 4, 1996 (received for review December 27, 1995)

ABSTRACT **The islet in non-insulin-dependent diabetes mellitus (NIDDM) is characterized by loss of β cells and large local deposits of amyloid derived from the 37-amino acid protein, islet amyloid polypeptide (IAPP). We have hypothesized that IAPP amyloid forms intracellularly causing β-cell destruction under conditions of high rates of expression. To test this we developed a homozygous transgenic mouse model with high rates of expression of human IAPP. Male transgenic mice spontaneously developed diabetes mellitus by 8 weeks of age, which was associated with selective β-cell death and impaired insulin secretion. Small intra- and extracellular amorphous IAPP aggregates were present in islets of transgenic mice during the development of diabetes mellitus. However, IAPP derived amyloid deposits were found in only a minority of islets at ≈20 weeks of age, notably after development of diabetes mellitus in male transgenic mice. Approximately 20% of female transgenic mice spontaneously developed diabetes mellitus at 30+ weeks of age, when β-cell degeneration and both amorphous and amyloid deposits of IAPP were present. We conclude that overexpression of human IAPP causes β-cell death, impaired insulin secretion, and diabetes mellitus. Large deposits of IAPP derived amyloid do not appear to be important in this cytotoxicity, but early, small amorphous intra- and extracellular aggregates of human IAPP were consistently present at the time of β-cell death and therefore may be the most cytotoxic form of IAPP.**

Non-insulin-dependent diabetes mellitus (NIDDM) is characterized by β-cell destruction and islet amyloid derived from islet amyloid polypeptide (IAPP) (1, 2). IAPP is a 37-amino acid protein that possesses amyloidogenic properties in species that spontaneously develop NIDDM (humans, monkeys, cats), but is non-amyloidogenic in mice that do not develop NIDDM (3, 4). Overexpression of human IAPP (h-IAPP), but not rat IAPP, in COS cells resulted in intracellular IAPP amyloidosis that was associated with cell death (5). Thus far, hemizygous transgenic mice for h-IAPP have not been reported to develop islet amyloid or diabetes mellitus spontaneously (6–8). Induction of marked insulin resistance in hemizygous mice transgenic for h-IAPP provokes intra- and extracellular IAPP amyloid formation, which is associated with β-cell death and hyperglycemia (9).

Based on these observations, we hypothesized that sufficiently increased rates of h-IAPP expression and synthesis results in intracellular IAPP amyloidosis and β-cell death, which results in diabetes mellitus (10). To examine this further, we developed a homozygous line of mice transgenic for h-IAPP, thereby doubling the h-IAPP gene copy number. We report here that these mice spontaneously developed diabetes mellitus due to β-cell death, which was associated with abnormal intra- and extracellular aggregates of h-IAPP. We conclude that overproduction of IAPP in vulnerable species (humans, monkeys, cats) may cause β-cell destruction and diabetes mellitus.

The publication costs of this article were defrayed in part by page charge payment. This article must therefore be hereby marked "*advertisement*" in accordance with 18 U.S.C. §1734 solely to indicate this fact.

MATERIALS AND METHODS

Preparation of Transgenic Construct. The RIPHAT transgene (2395 bp) is described elsewhere (9). It consists of a PCR-generated cDNA encompassing the h-IAPP coding sequence (270 bp) under the regulation of the rat insulin II promoter/5′ untranslated region and followed by intron I (728 bp) from the human albumin gene and the polyadenylylation site/RNA termination region (525 bp) from the human glyceraldehyde-3-phosphate gene (GAPDH). Use of the albumin intron I and GAPDH polyadenylylation site in transgenic constructs has been described (11).

Generation of Transgenic Mice. Hemizygotes of the RHF line described in Couce *et al.* (9) were self-crossed to generate F1 offspring. Transgenic offspring were identified by PCR amplification of RIPHAT from tail DNA. Hemizygotes were distinguished from homozygotes by backcross breeding to nontransgenic FVB/N mice. Homozygotes were defined as those mice that generated more than 20 transgenic and no nontransgenic offspring. Four such homozygotes were used to establish the core RHF breeding colony.

Northern Blot Analysis. Total RNA was prepared from whole pancreata of FVB/N, RHF hemizygote, and RHF homozygote males and females. Gels and blots were prepared and hybridized as described (9).

Study Design. *Protocol I.* To determine the impact of the homozygous h-IAPP state, the fasting blood glucose concentration was measured in 186 mice sacrificed by decapitation at 4–16 weeks of age. Fed plasma insulin and IAPP concentrations were measured in 58 transgenic and 70 control mice sacrificed at 8 and 16 weeks of age. Because the IAPP assay requires relatively large volumes of plasma, plasma samples were pooled from 3 to 5 mice to obtain a single IAPP concentration.

Protocol IIa. Having established that male transgenic mice spontaneously developed diabetes mellitus at approximately 8–12 weeks of age, which was characterized by impaired insulin secretion, we sought to examine the evolution of any abnormality in islet morphology at the level of light and electron microscopy by sequentially sacrificing 38 transgenic versus 38 nontransgenic mice at 2-week intervals between 5 and 26 weeks of age. Fed blood glucose concentrations were obtained from each mouse prior to sacrifice.

Protocol IIb. Having subsequently observed that 20% of female transgenic mice had developed diabetes mellitus at 30+ weeks of age, an additional five transgenic (selected as dia-

Abbreviations: NIDDM, non-insulin-dependent diabetes mellitus; IAPP, islet amyloid polypeptide; h-IAPP, human IAPP.

§To whom reprint requests should be addressed at: Department of Medicine, The University of Edinburgh, Western General Hospital, Edinburgh EH4 2XU, Scotland.

betic) and five nontransgenic female mice were sacrificed at between 36 and 41 weeks of age. Fed blood glucose concentrations were obtained prior to sacrifice and islet morphology was examined.

Assays. Glucose concentrations were measured by the glucose oxidase method using a One Touch II Glucometer (Lifescan, Milpitas, CA). Plasma insulin and IAPP concentrations were measured as described elsewhere (9, 12).

Light Microscopy. Mice were anesthetized by intraperitoneal injection of 3.2 mg of pentobarbital. A sample of the tail of the pancreas was fixed in neutral buffered formalin for 6 hr, dehydrated in ethanol, embedded in paraffin, sectioned, and stained for Congo red. In addition, deparaffinized sections were incubated in 5% goat serum/PBS/0.5% Tween 20 and stained with the peroxidase/anti-peroxidase method for insulin: guinea pig anti-porcine insulin 1:400 (Dako), biotinylated goat anti-guinea pig IgG 1:400 (Vector Laboratories), peroxidase-conjugated streptavidin 1:500 (Dako), stained with 3-amino-9-ethylcarbazole solution and counterstained with hematoxylin.

For a combined stain for glucagon and somatostatin, deparaffinized sections were treated with 1.5% hydrogen peroxide/50% methanol to block endogenous peroxidase activity, followed by 0.4% pepsin/0.01 N HCl, incubated in 5% goat serum/PBS/0.5% Tween 20, and stained with the peroxidase/anti-peroxidase method using a mixture of rabbit anti-human glucagon and rabbit anti-human somatostatin both at 1:400 (Dako) as primary antibodies.

Morphometric Analysis. Morphometric analysis was performed by use of an automated image analysis system as described (13) (Image-1 system, Universal Imaging, West Chester, PA). Because the β cells in the male transgenic mice became markedly degranulated (*vida infra*), direct imaging of insulin positive cells to estimate β-cell area would lead to an underestimate of this area in transgenic mice and an exaggerated estimate of the effect of the transgenic state on β-cell death.

To avoid this error, we calculated the islet β-cell area by subtracting the area occupied by α and δ cells from the total islet area in each islet examined. The resulting calculated β-cell area would tend, if anything, to underestimate the effect of the transgenic state on β-cell destruction since the calculated area includes some capillaries and connective tissue. Since the islet area occupied by α and δ cells was no different in transgenic and nontransgenic mice, and did not change over the period of observation, we calculated the ratio of the α and δ cell area compared with the total islet area. The latter ratio reduces the variability in measured islet area that results from the sectioning of islets at different tangents so that in the absence of selective β-cell destruction it remains relatively constant.

Electron Microscopy. Several 1-mm^3 samples from the tail of the pancreas were fixed in Trump's solution for 3 hr, and either postfixed in 1% OsO_4, block stained with 2% uranyl acetate, dehydrated using ethanol, and embedded in Spurr resin (14), or dehydrated with acetone and embedded in Quetol resin. Thin sections were etched with saturated sodium-m-periodate for 30 min, incubated in Tris-buffered saline (TBS)/0.1% (vol/vol) Tween 20/1% (vol/vol) goat serum/1% (wt/vol) ovalbumin/0.15 M glycine and immunagold labeled for IAPP: rabbit anti-human IAPP 1:1500 (Peninsula Laboratories) in TBS at 37°C for 2 hr; donkey anti-rabbit-immunoglobulin conjugated to 12 nm colloidal gold 1:300 (Jackson ImmunoResearch) in TBS/Tween for 1.5 hr. Sections were counterstained for 15 min in uranyl acetate (Quetol only) and for 5 min in lead citrate.

Statistical Analyses. Data are presented as mean ± SEM (Figs. 1 *B* and *C*, and 2*B*, and Protocol IIb) or individual data points (Fig. 2). Comparison of the insulin and IAPP concentrations between transgenic and nontransgenic mice were made by a nonpaired, two-tailed Student's *t* test. Comparison of the blood glucose concentrations with aging was made by use of ANOVA (Protocol I), multiple regression analysis (Protocol IIa), and nonpaired, one-tailed Student's *t* test (Protocol IIb). The relationship between the total islet area, the calculated β-cell area, and the fractional islet area occupied by α and δ cells versus weeks of age were examined by regression analyses. A P value of < 0.05 was taken as evidence of significant difference.

RESULTS

Protocol I. Hemizygous mice of the RHF line did not develop any diabetic phenotype or glucose intolerance at any age (up to 2 years). A homozygous line was established to increase the expression level of the transgene. Northern blot analysis of the resulting mice showed at least a 35% increase of mRNA in males and a 75% increase in females compared with their hemizygous counterparts (Fig. 1*A*). Between 4 and 8 weeks of age, male transgenic mice spontaneously developed diabetes mellitus (Fig. 1*B*). Female transgenic mice developed mild hyperglycemia during the 16-week period of observation (Fig. 1*B*). The plasma insulin concentration was comparable in transgenic and control mice at 8 weeks of age (both sexes). In contrast, by 16 weeks of age in male transgenic mice, plasma insulin concentrations were markedly lower ($P < 0.01$) than in controls, despite severe hyperglycemia, implying a major β-cell defect (Fig. 1*C*). If untreated, after ≈16 weeks of age, many male transgenic mice died, presumably as a consequence of marked hyperglycemia. At 16 weeks of age, the plasma insulin concentrations in female transgenic mice were comparable to those in nontransgenic mice despite the presence of mild hyperglycemia, implying a more subtle defect of insulin secretion in the female transgenic mice. Plasma IAPP concentrations were comparably elevated in female transgenic mice, compared with female nontransgenic mice, at 8 and 16 weeks of age (Fig. 1*C*). Plasma IAPP concentrations in male transgenic versus nontransgenic mice fell from 8 to 16 weeks of age in parallel with the insulin concentrations (Fig. 1*C*). This phenotype is not due to an insertion mutation because we also observe comparable hyperglycemia in two independent lines of transgenic rats generated with the same transgene.

Protocol IIa. Inspection of the islet of Langerhans by light microscopy indicated that the cross-sectional islet area was comparable in transgenic and nontransgenic mice at 5 weeks of age. However, the mean islet area decreased significantly ($P < 0.05$) in male transgenic mice (slope = -0.48×10^3 μm^2 per week), but not in female transgenic mice (slope = 0.13×10^3 μm^2 per week) or control mice (slope = 0.22×10^3 μm^2 per week) during the period of observation (see Fig. 3). Morphometric analysis confirmed that this decreased islet area in male transgenic mice was due to decreased β cells since there was a corresponding decrease ($P < 0.05$) in the calculated β-cell islet area in the male transgenic mice (slope -0.50×10^3 μm^2 per week), but not the female transgenic mice (slope = 0.10×10^3 μm^2 per week) or control mice (slope = 0.21×10^3 μm^2 per week). The selective destruction of β cells in the male transgenic mice is clearly depicted by the positive deflection of the fraction of total islet area occupied by α and δ cells (Fig. 2). The onset of this increase at ≈12 weeks of age coincided with, or was perhaps slightly later than, the steep increase in the blood glucose concentration that occurred at ≈10 weeks of age in these mice (Fig. 2). Furthermore, the location of α and δ cells within an islet cross section in male or female transgenic mice appeared to encroach from the classical peripheral distribution to within the core of the islet when compared with the pattern of cellular distribution in the control mice (Fig. 3 *D* versus *E*).

Examination of islets of transgenic mice by electron microscopy showed five distinct features. (*i*) The first and most striking abnormality detected was the frequent presence of

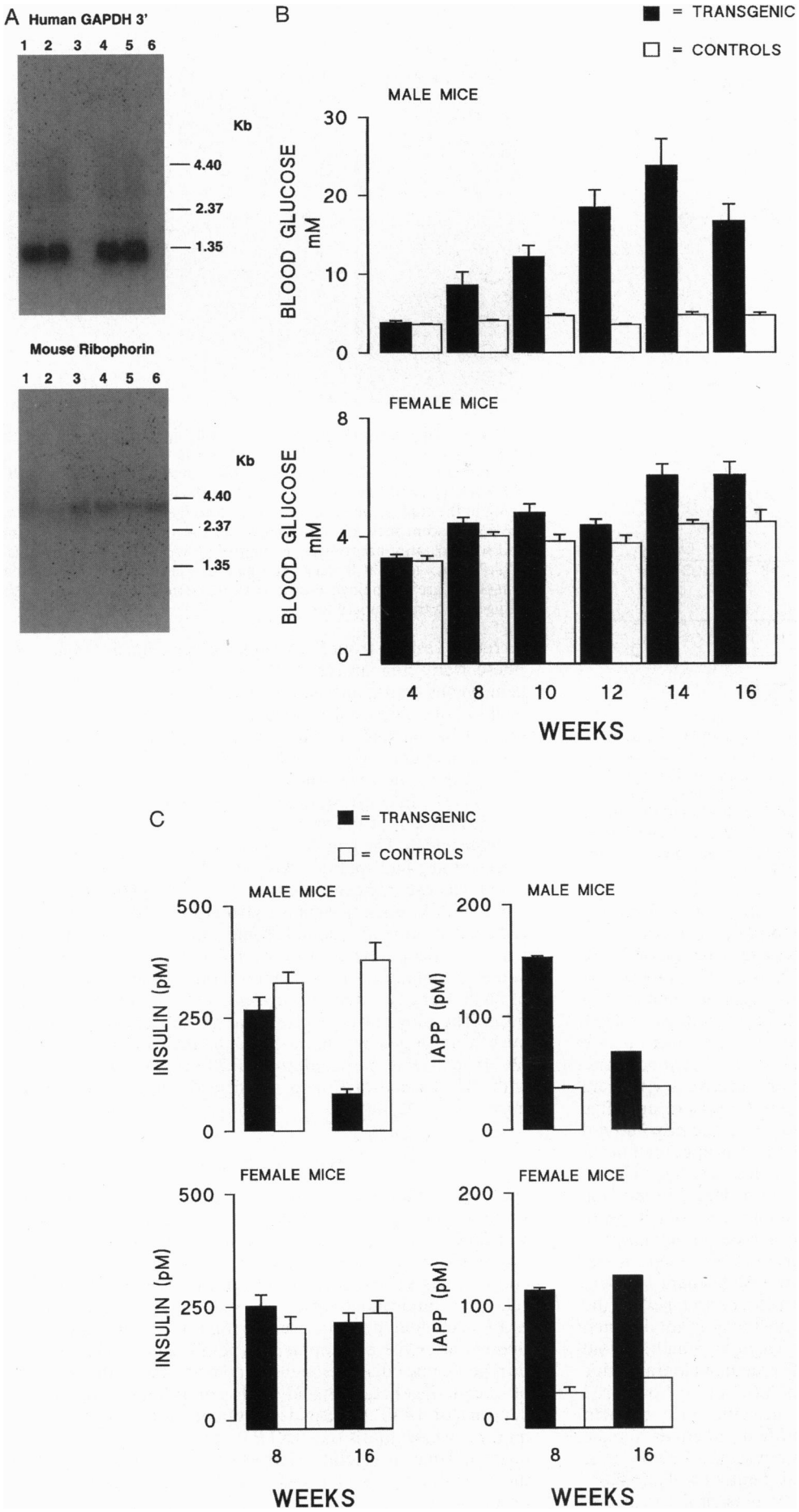

FIG. 1. (*A*) Transgene expression in pancreata from the nontransgenic FVB/N background strain and from transgenic hemizygote and homozygote mice. Twin blots were prepared from two separate gels loaded with identical amounts of total RNA (25 μg) in each lane. Lanes 1–3 males, lanes 4–6 females; lanes 1 and 4, h-IAPP transgenic hemizygote; lanes 2 and 5, h-IAPP transgenic homozygote; lanes 3 and 6, FVB/N background strain. (*Top*) Hybridization to the human GAPDH 3′ untranslated region portion of the RIPHAT transgene. (*Bottom*) Hybridization to murine ribophorin cDNA. Quantitation of mRNA levels in hemizygous versus homozygous mice by phosphorimager analysis and normalization to ribophorin expression levels indicated that transgene mRNA levels were 35% (males) to 75% (females) higher in the homozygous animals. (*B*) Fasting blood glucose concentrations in h-IAPP transgenic (solid bars) and nontransgenic (open bars) male (*top*) and female (*bottom*) mice. The blood glucose concentrations were significantly higher in h-IAPP transgenic versus nontransgenic mice ($P < 0.001$, both male and female) from 8 weeks of age in male mice and 14 weeks of age in female mice (Bonferroni multiple comparison procedure). (*C*) Fed plasma insulin (*left*) and IAPP (*right*) concentrations in male (*top*) and female (*bottom*) h-IAPP transgenic (solid bars) and nontransgenic (open bars) mice at 8 and 16 weeks of age. The plasma insulin concentrations were significantly lower in male h-IAPP transgenic versus male nontransgenic mice at 16 weeks of age ($P < 0.01$), but there was no significant difference between female transgenic versus nontransgenic mice. The plasma IAPP concentrations were significantly increased in transgenic versus nontransgenic mice at 8 weeks of age.

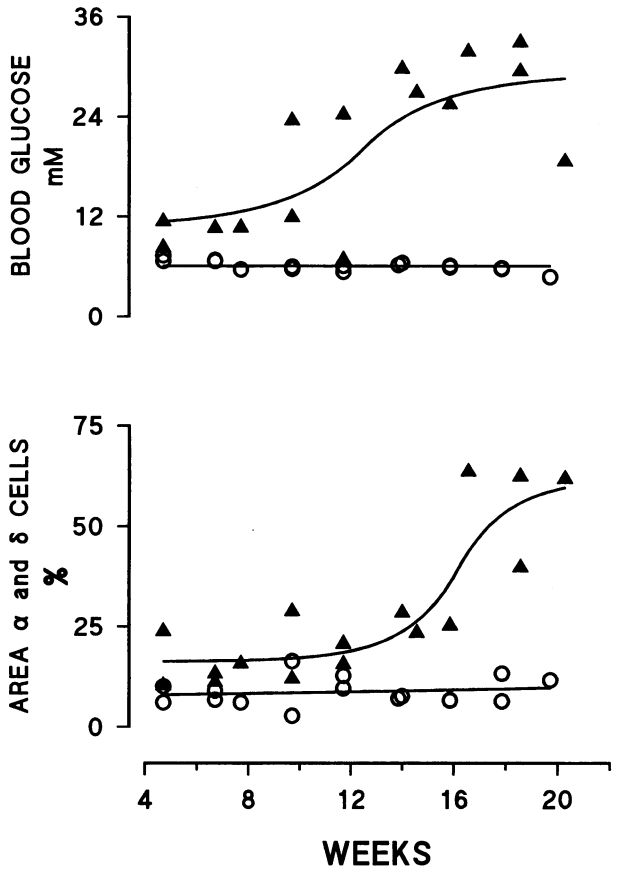

FIG. 2. Fed blood glucose concentrations (*top*) and mean percentage of non-β-cell area to total islet area (*bottom*) obtained from the same mice at the time of sacrifice. All data shown in this figure are from male h-IAPP transgenic (solid triangles) and male nontransgenic (open circles) mice. Multiple regression analysis indicated that blood glucose concentrations were increased ($P < 0.001$) in h-IAPP male transgenic mice, and that the fractional islet area occupied by α and δ cells was increased ($P < 0.001$) in the same mice.

degenerative β cells in male transgenic mice (Fig. 4*A*) starting at 8 weeks of age consistent with the morphometric assessment at light microscopy that implied selective destruction of β cells in male transgenic mice (Fig. 2). Non-β cells showed no degeneration consistent with the increased fractional area of the islet occupied by non-β cells as diabetes mellitus evolved. In female transgenic mice degenerative β cells were a rare finding at the age of 5–26 weeks. (*ii*) Small intra- and extracellular amorphous deposits of immunoreactive IAPP were observed in male transgenic mice from 8 weeks of age (Fig. 4*B*). Most deposits were present inside or in the proximity of degenerative β cells. The majority of deposits appeared intracellular and were associated with vacuoles, vesicles, or cytoplasm as far as could be established in a degenerating cell. Perivascular accumulations of immunoreactive IAPP were very small compared with those observed in hemizygous transgenic mice made insulin resistant (9). In female transgenic or control mice no intra- or extracellular deposits were present during the 5–26 week observation period. (*iii*) In the majority of the male transgenic mice amyloid was not detected despite extensive β-cell degenerative changes. Small amyloid deposits of IAPP were only rarely observed in male transgenic mice at 20 weeks of age (Fig. 4 *C* and *D*), but no Congo red deposits were identified in male transgenic mice by light microscopy. Amyloid was not identified in either female transgenic or control mice aged 5–26 weeks. (*iv*) In both male and female transgenic mice abnormal, faintly fibrillar (diameter 8–10 nm) aggregates of IAPP were present in the insulin

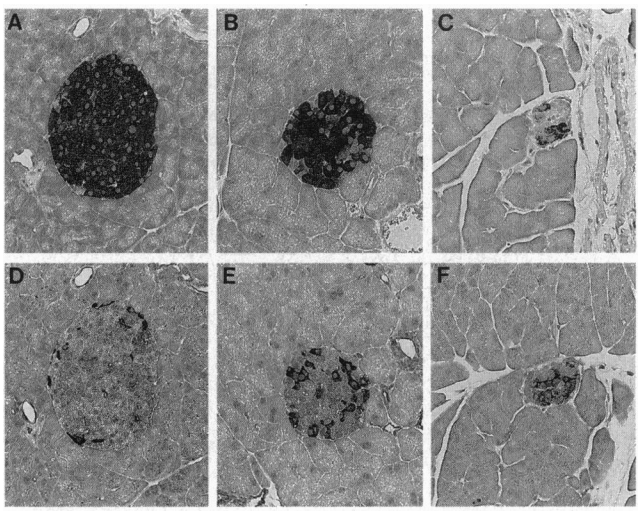

FIG. 3. Islet morphology of male mice by light microscopy. (*A–C*) Representative islets stained for insulin (dark is positive) from a nontransgenic control (16 weeks old) (*A*) versus transgenic for h-IAPP at 8 weeks (*B*) and 16 weeks (*C*). Note that the islet size decreased with aging in the transgenic mice due to reduced insulin positive cell area. (*D–F*) Adjacent sections of the same islets stained for both glucagon and somatostatin: nontransgenic control 16 weeks of age (*D*) versus h-IAPP transgenic at 8 weeks (*E*) and 16 weeks (*F*). Note that the non-β-cell area remained constant as the β-cell area declined with aging in the transgenic mice.

secretory vesicles from 5–26 weeks of age (Fig. 5 *A* versus *B*). These were comparable to those described previously in a hemizygous transgenic mouse that did not develop diabetes mellitus (8). These intravesicular IAPP aggregates were not present in controls. (*v*) There was a marked decrease in the cytoplasmic density of insulin secretory vesicles (degranulation) in the male transgenic mice from 8 weeks of age (Fig. 5 *C* versus *D*). In contrast, in female mouse islets degranulation was not present at the same age.

Protocol IIb. The female transgenic mice sacrificed at 36–41 weeks of age had spontaneously developed diabetes mellitus, blood glucose concentration 15.3 ± 4.2 versus 5.3 ± 0.1 mmol/liter (transgenic versus controls; $P < 0.05$). Small Congo red deposits were identified in some female transgenic islets by light microscopy. By electron microscopy β-cell degeneration and degranulation, and both amorphous and amyloid deposits of IAPP were detected in transgenic but not in nontransgenic mice. The amyloid deposits found in the female transgenic mice were larger and more frequent than those only rarely observed in male transgenic mice at 20 weeks of age, consistent with the absence of Congo red deposits in male transgenic mice.

DISCUSSION

We report that homozygous transgenic mice for h-IAPP spontaneously developed diabetes mellitus; males at ≈8 weeks and 20% of females by 30 or more weeks of age. In male transgenic mice diabetes mellitus was characterized by decreased plasma insulin concentrations, selective death of β cells, and amorphous intra- and extracellular aggregates of IAPP. Amyloid deposits were a relatively late and sparse finding, after the development hyperglycemia. In the female transgenic mice diabetes mellitus coincided with the presence of β-cell degeneration and both amorphous and amyloid deposits of IAPP. These data support the hypothesis that marked oversynthesis of h-IAPP by β cells may lead to β-cell death and diabetes mellitus. However, the mechanism by which the overproduction of h-IAPP leads to cell death remains uncertain.

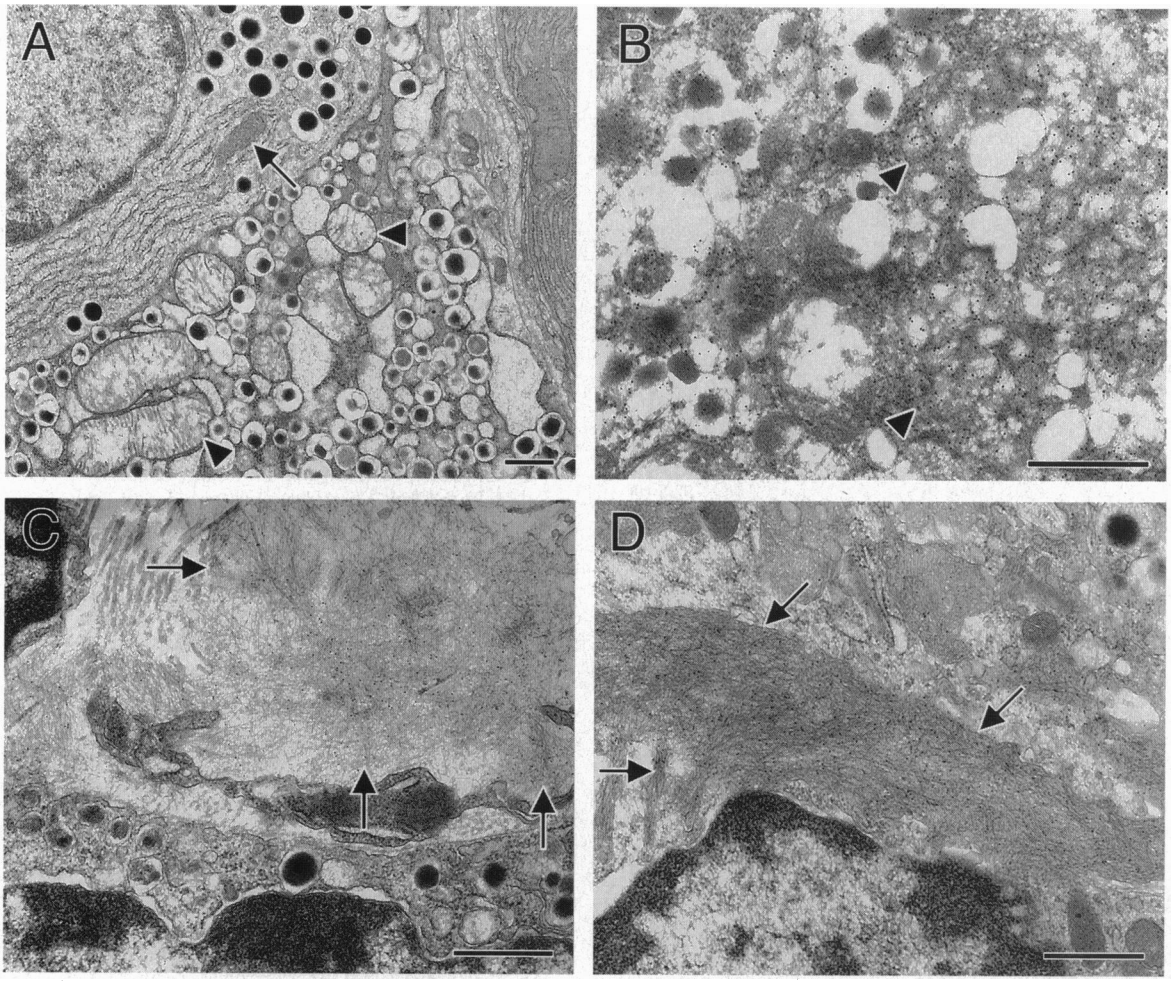

FIG. 4. Islet ultrastructure of h-IAPP transgenic male mice. (*A*) Part of a degenerative β cell containing swollen mitochondria (central cell, arrowheads). In contrast, a neighboring α cell contains normal mitochondria (top left cell, arrow) and rough endoplasmic reticulum as does adjacent exocrine tissue (right). (*B*) Amorphous deposit immunoreactive for IAPP (arrowheads) in a transgenic mouse 10 weeks of age. (*C*) Extracellular amyloid (arrows) immunogold labeled for IAPP in a male transgenic mouse 20 weeks of age. (*D*) Intracellular amyloid deposit immunoreactive for IAPP (arrows) present in close proximity to the β-cell nucleus in a male transgenic mouse 20 weeks of age. (Bars = 0.5 μm.)

Extra- and intracellular IAPP-derived amyloid deposits have previously been associated with cell death (5, 9, 15–17). However, the observations in male transgenic mice in which β-cell death was extensive when amyloid was rare or absent imply that extensive IAPP-derived amyloid deposits are not necessary for IAPP to cause β-cell death. Furthermore, in insulinoma tissue (18) and diabetes mellitus (7) extensive extracellular amyloid deposits can be observed adjacent to healthy β cells, arguing against toxicity of large deposits of extracellular fibrils. In islets of female transgenic mice that developed diabetes mellitus, more frequent and extensive amyloid was observed. Thus, amyloid does not appear necessary for IAPP induced β-cell death.

Another possibility is that the h-IAPP expressed in the transgenic mice had a direct cytotoxic effect in its soluble form. In support of this is the observation that h-IAPP, but not rat IAPP, is cytotoxic when applied to fetal hippocampal cells (16) and β cells (17). However, because neither rat IAPP nor the sequence of h-IAPP that differs from rat $IAPP_{20-29}$ were cytotoxic (16), it would appear that h-IAPP is probably only cytotoxic in the structural conformation of β-pleated sheet polymers. The fact that other structurally unrelated amyloidogenic peptides have also been shown to be cytotoxic through a similar mechanism (19) supports the key role of the β-pleated sheet structure in cytotoxicity.

If h-IAPP is only toxic in the fibrillar form, then why is β-cell degeneration present in male transgenic mice from 8 weeks of age in the absence of detectable amyloid? Little is yet known about the relationship between the size of amyloid fibrils and their cytotoxicity, and it is quite plausible that small fibrils are more cytotoxic than large fibrils. It has recently been reported that maturation of amyloid β protein into extensive amyloid fibrils negates their cytotoxic properties (20). Small intra- and extracellular amorphous deposits of IAPP, which may represent aggregates of immature IAPP fibrils, were present at the same time as β-cell death in both the male and the female transgenic mice. However, it is not possible to distinguish whether these amorphous IAPP aggregates cause or are due to β-cell degeneration.

Distinct from amyloid and amorphous deposits of IAPP we observed IAPP immunoreactive aggregates confined to the secretory vesicles in transgenic mice. However, similar intravesicular deposits are reported elsewhere in hemizygous h-IAPP transgenic mice that did not develop diabetes mellitus (8) and these deposits were not related temporally to cell death in the present study. It is therefore unlikely that these intravesicular aggregates of IAPP were responsible for β-cell death in male transgenic mice.

Another interesting observation in the present study is the relatively late onset of diabetes mellitus in female versus male transgenic mice. The appearance of the diabetes mellitus phenotype in several mouse models is sexually dimorphic, affecting males more than females (21–23), consistent with the present study. This sexual dimorphism appears to be due to the

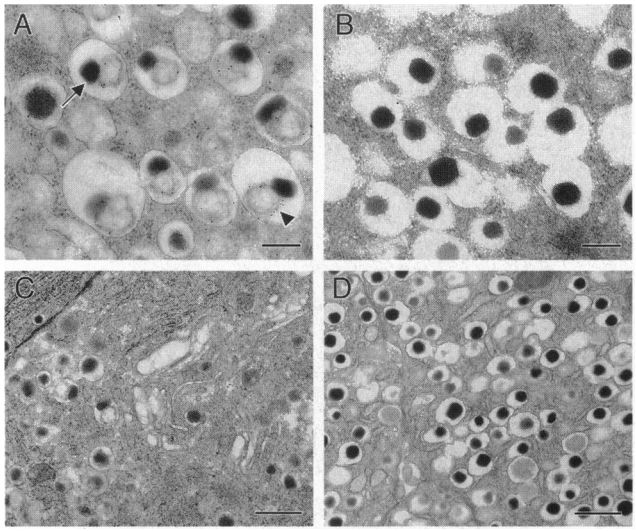

FIG. 5. Typical ultrastructure of h-IAPP transgenic and nontransgenic mouse β cells. (*A*) In a female h-IAPP transgenic mouse at 16 weeks of age the insulin secretory vesicles contain a dense core of insulin (arrow) and a faintly fibrillar structure immunoreactive for IAPP (arrowhead). The dense core commonly appears to have been displaced from the fibrillar material that previously surrounded it. (*B*) At the same magnification as *A*, the faintly fibrillar structure immunoreactive for IAPP is absent in a nontransgenic female mouse 26 weeks of age. (*C*) β-cell degranulation in a male transgenic mouse 12 weeks of age. Note the fibrillar material in the insulin secretory vesicles. (*D*) At the same magnification as *C*, the cytoplasm of a nontransgenic male mouse 12 weeks of age is packed with insulin secretory vesicles. (Bars = 0.2 μm in *A* and *B*; 0.5 μm in *C* and *D*.)

divergent effects of estrogens versus androgens on hepatic estrogen sulfotransferase (23). The latter most likely acts by causing relative insulin resistance in male versus female mice, an effect that would be expected to enhance development of diabetes mellitus in male mice in the present model.

In conclusion, we report a homozygous transgenic mouse model for h-IAPP that spontaneously develops diabetes mellitus associated with abnormal aggregates of IAPP and β-cell degeneration. This mouse model provides an important tool to investigate the role of IAPP in the pathogenesis of islet dysfunction in NIDDM.

We thank Jeff Stock for microinjection of the RIPHAT transgene and founder animal generation. We acknowledge the excellent technical assistance of Maynard Carty, Steve Orena, Ann Brodeur, Karen Laakso, Jane Kahl, Joyce Sackett, and Steve Ziesmer. We also thank Paul McGill of the Pfizer Animal Resources Department for the supervision of the animal breeding. We appreciate the invaluable suggestions and guidance of Drs. Susan Bonner-Weir and Gordon Weir (Joslin Diabetes Center) and Drs. David Toft and Norman Eberhardt (Mayo Clinic) in the design and methodology of the present studies. These studies were funded in part by grants from the U.S. Public Health Service (DK-44341), Pfizer Inc., and the Mayo Foundation.

1. Johnson, K. H., O'Brien, T. D., Betsholtz, C. & Westermark, P. (1989) *N. Engl. J. Med.* **321,** 513–518.
2. Johnson, K. H., O'Brien, T. D., Betsholtz, C. & Westermark, P. (1992) *Lab. Invest.* **66,** 522–535.
3. Betsholtz, C., Christmansson, L., Engström, U., Rorsman, F., Svensson, V., Johnson, K. H. & Westermark, P. (1989) *FEBS Lett.* **251,** 261–264.
4. Ohagi, S., Nishi, M., Bell, G. I., Ensinck, J. W. & Steiner, D. F. (1991) *Diabetologia* **34,** 555–558.
5. O'Brien, T. D., Butler, P. C., Kreutter, D. K., Kane, L. A. & Eberhardt, N. L. (1995) *Am. J. Pathol.* **147,** 609–616.
6. Fox, N., Schrementi, J., Nishi, M., Ohagi, S., Chan, S. J., Heisserman, J. A., Westermark, G. T., Leckström, A., Westermark, P. & Steiner, D. F. (1993) *FEBS Lett.* **323,** 40–44.
7. de Koning, E. J. P., Höppener, J. W. M., Verbeek, J. S., Oosterwijk, C., van Hulst, K. L., Baker, C. A., Lips, C. J. M., Morris, J. F. & Clark, A. (1994) *Diabetes* **43,** 640–644.
8. Yagui, K., Yamaguchi, T., Kanatsuka, A., Shimada, F., Huang, C. I., Tokuyama, Y., Ohsawa, H., Yamamura, K.-I., Miyazaki, J.-I., Mikata, A., Yoshida, S. & Makino, H. (1995) *Eur. J. Endocrinol.* **132,** 487–496.
9. Couce, M., Kane, L. A., O'Brien, T. D., Charlesworth, J., Soeller, W., McNeish, J., Kreutter, D., Roche, P. & Butler, P. C. (1996) *Diabetes,* in press.
10. Butler, P. C., Eberhardt, N. L. & O'Brien, T. D. (1994) in *Molecular Biology of Diabetes, Part I,* eds. Drazin, B. & LeRoith, D. (Humana, Totowa, NJ), pp. 381–398.
11. Marshall, B. A., Ren, J.-M., Johnson, D. W., Gibbs, E. M., Lillquist, J. S., Soeller, W. C., Holloszy, J. O. & Mueckler, M. (1993) *J. Biol. Chem.* **268,** 18842–18445.
12. Butler, P. C., Chou, J., Carter, W. B., Wang, Y.-N., Bu, B.-H., Chang, D., Chang, J.-K. & Rizza, R. A. (1990) *Diabetes* **39,** 752–756.
13. Couce, M., O'Brien, T. D., Moran, A., Roche, P. C. & Butler, P. C. (1996) *J. Clin. Endocrinol. Metab.* **81,** 1267–1272.
14. Spurr, A. R. (1969) *J. Ultrastruc. Res.* **71,** 173–184.
15. Westermark, P. (1973) *Virchows Archiv. A* **359,** 1–18.
16. May, P. C., Boggs, L. N. & Fuson, K. S. J. (1993) *Neurochemistry* **61,** 2330–2333.
17. Lorenzo, A., Razzaboni, B., Weir, G. C. & Yankner, B. A. (1994) *Nature (London)* **368,** 756–760.
18. O'Brien, T. D., Butler, A. E., Roche, P. C., Johnson, K. H. & Butler, P. C. (1994) *Diabetes* **43,** 329–336.
19. Schubert, D., Behl, C., Lesley, R., Brack, A., Dargusch, R., Sagara, Y. & Kimura, H. (1995) *Proc. Natl. Acad. Sci. USA* **92,** 1989–1993.
20. Davis-Salinas, J. & Van Nostrand, W. E. (1995) *J. Biol. Chem.* **270,** 20887–20890.
21. Efrat, S., Fleischer, N. & Hanahan, D. (1990) *Mol. Cell. Biol.* **10,** 1779–1783.
22. Allison, J., Malcolm, L., Culvenor, J., Bartholomeusz, R. K., Holmberg, K. & Miller, J. F. A. P. (1991) *Proc. Natl. Acad. Sci. USA* **88,** 2070–2074.
23. Gill, A. M., Leiter, E. H., Powell, J. G., Chapman, H. D. & Yen, T. T. (1994) *Diabetes* **43,** 999-1004.